Vitrification of octonary perylene mixtures with ultralow fragility

APPLIED SCIENCES AND ENGINEERING

Vitrification of octonary perylene mixtures with ultralow fragility

Sandra Hultmark[1], Alex Cravcenco[2], Khushbu Kushwaha[2], Suman Mallick[2], Paul Erhart[3], Karl Börjesson[2], Christian Müller[1]*

Strong glass formers with a low fragility are highly sought-after because of the technological importance of vitrification. In the case of organic molecules and polymers, the lowest fragility values have been reported for single-component materials. Here, we establish that mixing of organic molecules can result in a marked reduction in fragility. Individual bay-substituted perylene derivatives display a high fragility of more than 70. Instead, slowly cooled perylene mixtures with more than three components undergo a liquid-liquid transition and turn into a strong glass former. Octonary perylene mixtures display a fragility of 13 ± 2, which not only is a record low value for organic molecules but also lies below values reported for the strongest known inorganic glass formers. Our work opens an avenue for the design of ultrastrong organic glass formers, which can be anticipated to find use in pharmaceutical science and organic electronics.

INTRODUCTION

Vitrification, the conversion of a material into a noncrystalline glassy solid, is important for many types of materials from SiO_2, bulk metallic glasses (*1*), amorphous pharmaceutical formulations (*2*), and protein drugs (*3*) to organic semiconductors used for organic light-emitting diodes (*4*) and solar cells (*5*). Hence, concepts that facilitate the design of materials with a high glass-forming ability are in high demand. The tendency of a material to adopt a glassy state devoid of any crystalline domains depends on thermodynamic as well as kinetic factors, which influence the rate of crystal nucleation as well as growth between the glass transition and melting temperature, T_g and T_m. There are numerous factors that influence the overall tendency for crystallization, and theoretical as well as experimental studies have discussed the influence of, e.g., the thermodynamic driving force for crystallization, the reduced glass transition temperature $T_{rg} = T_g/T_m$, and the temperature dependence of the diffusion rate D and, hence, viscosity η above T_g (assuming that the Stokes-Einstein relation holds, i.e., $D \propto \eta^{-1}$) (*6*).

Multicomponent mixtures are widely used for promoting glass formation because mixing reduces the thermodynamic driving force for crystallization (*2*, *7*, *8*). The impact of mixing on the kinetic factors that determine glass formation is a subject of much ongoing research (*9*, *10*). The cooling rate needed to avoid crystallization and, instead, reach a glassy state depends on the temperature dependence of the viscosity above T_g, which affects the ability of molecules to form crystal nuclei and later reach the growing crystal. How rapidly the viscosity of a liquid increases during cooling is described by its kinetic fragility, which is a measure of the rate of change in η in the vicinity of T_g, expressed as $m = [d \log \eta/d(T_g/T)]_{T=T_g}$ (*11*, *12*).

The fragility has been measured for a myriad of organic molecules from fragile glass formers such as *o*-terphenyl with a high $m = 81$ (*13*) to strong glass formers such as *n*-propanol with $m = 35$, poly(ethylene oxide) (PEO) with $m = 23$ (*14*), and certain pharmaceutical compounds, some of which display very low fragilities down to $m = 18$ in the case of tolazamide (*6*). Some of the strongest inorganic glass formers are SiO_2, GeO_2, and BeF_2 with $m = 20$ (*15*). The lowest reported fragility of $m = 14$ has been measured for low-density amorphous water (*16*).

While the fragility of many organic molecules and polymers has been determined, less attention has been paid to the influence of mixing on the fragility. Some, but not all (*17*–*19*), two- or three-component systems feature a lower fragility than the individual components (*20*–*26*). A decrease in fragility upon mixing has been observed for a number of binary and ternary systems such as, e.g., mixtures of small molecules (including isomers) (*20*–*24*), additive-containing polymers such as antiplasticizers (*25*, *27*), solid electrolytes with a polymeric additive (*28*), and bimodal polystyrene (*26*). While the absolute effect of mixing on the fragility tends to be small, the tendency for crystallization can strongly decrease upon mixing of two components. For example, binary mixtures of the pharmaceutical compound celecoxib ($m = 89$) with octacetylmaltose display a 20% lower fragility compared to the neat components and do not undergo crystallization for at least 9 months (*24*). A more substantial change in fragility may open the possibility to design strong glass-forming materials with individually fragile compounds.

Here, we demonstrate that judicious mixing of up to eight different molecules, which, on their own, are relatively fragile materials with $m > 70$, results in a material with a record low kinetic fragility of only 13 ± 2. We achieve this unprecedented decrease in fragility by more than 500% through a systematic study of a series of binary to octonary perylene mixtures, which solely comprise carbon-based molecules that contain no heteroatoms or functional groups such as hydrogen-bonding moieties. While neat perylene displays a high tendency for crystallization and high $T_m = 278$°C, derivatives that carry alkyl substituents at one of the bay positions feature a much lower $T_m \leq 121$°C and cease to crystallize once mixed with a second derivative (*29*). Because of the low T_m of bay-substituted perylenes, which minimizes thermal degradation during thermal analysis experiments, as well as the easily discernible T_g, we chose to use a series of these derivatives as a model system to study the impact of mixing on the kinetic fragility. We find that the fragility of perylene mixtures continuously decreases with the number of components,

[1]Department of Chemistry and Chemical Engineering, Chalmers University of Technology, 41296 Göteborg, Sweden. [2]Department of Chemistry and Molecular Biology, University of Gothenburg, Kemigården 4, 41296 Göteborg, Sweden. [3]Department of Physics, Chalmers University of Technology, 41296 Göteborg, Sweden.
*Corresponding author. Email: christian.muller@chalmers.se

and systems that undergo a liquid-liquid transition display values that rival those of the strongest known glass formers.

RESULTS

We chose to work with a series of perylenes that carry a linear or branched alkyl group at one of the bay positions (Fig. 1). All eight materials readily crystallize when cast from solution and have melting temperatures between 56° and 121°C (table S1). We note that differential scanning calorimetry (DSC) cooling thermograms recorded at a rate of −0.17 K s^{-1} do not feature a crystallization exotherm, indicating that single bay-substituted perylenes already display a high tendency for glass formation. Crystallization is hindered because of the twisting of the conjugated core, which, in the case of perylene bisimides, is known to influence the aggregation behavior (*30*), and leads to the presence of two atropisomers for each of the bay-alkylated molecules (A to H) (see fig. S1 for the two atropisomers of perylene A) (*29*).

In a first set of experiments, we studied the impact of mixing on the reduced glass transition temperature, which is a measure of the narrowness of the temperature window $T_g < T < T_m$ where crystallization can occur. We focused on perylenes A, B, and C with ethyl, butyl, and hexyl pendant groups, which individually have a T_{rg} of about 0.7, and prepared binary and ternary mixtures with different stoichiometries. DSC first heating thermograms of solution-cast materials indicate that T_m decreases upon mixing, while T_g remains similar (table S1), resulting in a measurable but higher T_{rg} of up to 0.78 for all mixtures that are rich in either of the three components (Fig. 2). Instead, binary and ternary mixtures with a close-to-stoichiometric ratio do not undergo crystallization (and hence do not display a T_m), indicating an increased tendency for glass formation.

We went on to study the impact of mixing on the fragility and chose to focus on perylene mixtures that comprise an equal weight of each component. Fast scanning calorimetry (FSC) allowed us to study the impact of the cooling rate q on the fictive temperature T_f', which corresponds to the temperature where the liquid freezes into a glass. The material is first heated to 150°C to erase the thermal history, followed by cooling at −0.1 to −1000 K s^{-1} and lastly heating at 600 K s^{-1} (Fig. 3A). This cycle is repeated for each cooling rate. FSC heating thermograms display a pronounced enthalpy overshoot that increases in size as the absolute value of q decreases. In case of slow cooling, the material has more time to relax and hence requires more energy during reheating to regain its mobility and reach the liquid state (Fig. 3B). To determine T_f', we compared the difference of the heat capacity of the liquid and glassy states using the area matching method established by Moynihan *et al.* (*31*) for fast cooling rates and an extrapolation method for slow cooling rates, for which we observe that T_f' lies below the onset of devitrification (Fig. 3B; see Materials and Methods for details) (*32*, *33*). For the ABC ternary mixture, for instance, we observe that T_f' increases from −26° to −7.5°C as q changes from −0.1 to −1000 K s^{-1} (Fig. 3B).

We measured T_f' for a series of binary to octonary perylene mixtures using cooling rates from −0.1 to −1000 K s^{-1} and constructed a fragility plot that compares $-\log|q|$ with $T'_{f,ref}/T'_f$, where $T'_{f,ref}$ is obtained from DSC heating thermograms at 0.17 K s^{-1} (Fig. 4A). The fragility can then be extracted from the slope around the reference glass transition temperature, i.e., $m = -[d\log|q|/d(T'_{f,ref}/T'_f)]_{T'_{f,ref}=T'_f}$ (*33*, *34*). For all perylenes A to H, we observe a linear correlation between $-\log|q|$ and $T'_{f,ref}/T'_f$, the slope yielding fragilities of $m = 71$ to 97 (note that the lowest value of $m = 71$ was measured for G, which is a racemic mixture; fig. S2), similar to $m = 85$ for *o*-terphenyl, which we have evaluated as a reference compound (table S1). Binary and ternary mixtures likewise show a linear trend but yield lower fragilities of about 70 and 60, respectively, which confirms that mixing affects not only the thermodynamic but also the kinetic factors that influence glass formation. The slope of the fragility plot close to $T'_{f,ref} = T'_f$ continues to decrease with the number of components, yielding a value of $m < 20$ for the septenary and octonary mixtures, obtained from data collected at low cooling rates of $|q| \leq 5$ K s^{-1}

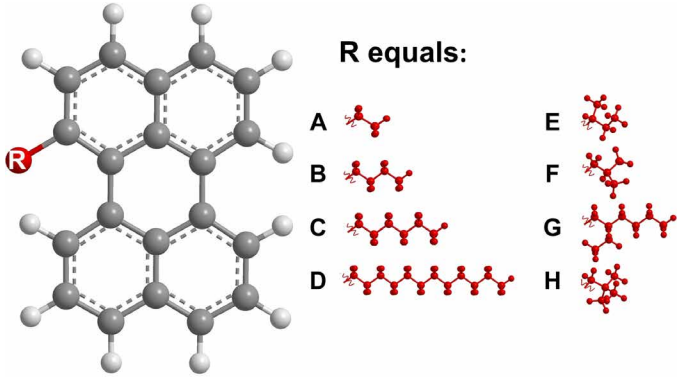

Fig. 1. Molecular structures of the bay-substituted perylenes with different pendant alkyl groups. The molecules are labeled A to H.

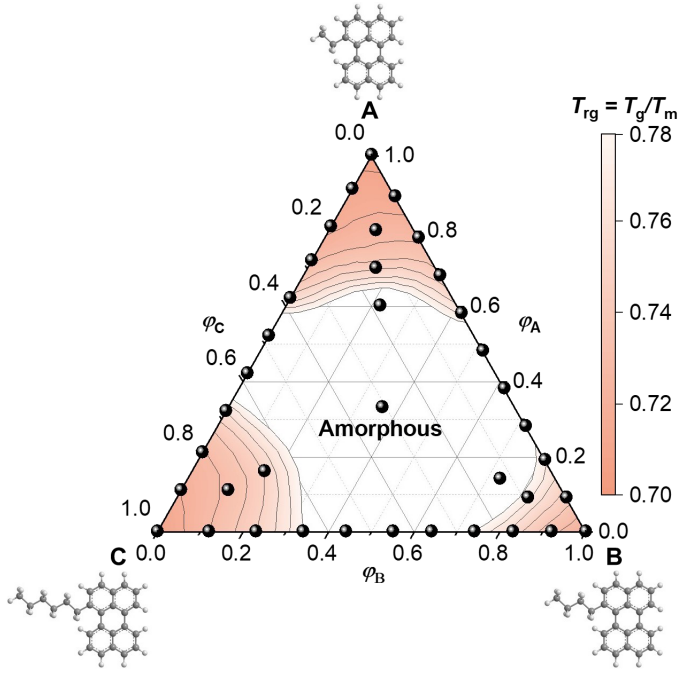

Fig. 2. Reduced glass transition temperature T_{rg} of ABC mixtures. T_{rg} of different stoichiometries (φ_A, φ_B, and φ_C are the molar fractions of compounds A, B, and C, respectively) was determined using the T_g and T_m values extracted from DSC first heating thermograms (0.17 K s^{-1}). Black circles indicate stoichiometries for which thermograms were recorded; the central white area corresponds to mixtures that remained amorphous.

(Fig. 4B). The fragility of the octonary mixture was extracted from three independent measurements, yielding a value of $m = 13 \pm 2$, which is lower than the values reported for the strongest known organic and inorganic glass formers, including tolazamide (*6*) and SiO_2 (*15*).

The fragility plots of mixtures with more than three components display a distinct change in slope when comparing data recorded for low and high cooling rates (Fig. 4A). The fragility plot of the octonary mixture, for example, reveals two distinct regimes with a shallow slope close to $T'_{f,ref} = T'_f$ for $|q| \leq 5\ K\ s^{-1}$ and a much steeper one for $|q| > 5\ K\ s^{-1}$, the latter of which is comparable to the slope observed for single perylenes. We propose that perylene mixtures undergo a liquid-liquid transition as long as the liquid is cooled at a sufficiently low rate. Fragility plots that feature a change in slope have been observed in the case of other materials such as water (*35*), SiO_2 (*36*), BeF_2 (*37*), $ZnCl_2$ (*38*), and different metallic glass-forming liquids (*39*–*41*). This type of behavior, which is often referred to as a fragile-to-strong transition, has been suggested to arise because the liquid adopts a new local structure and density, affecting the relaxation kinetics (*42*–*45*).

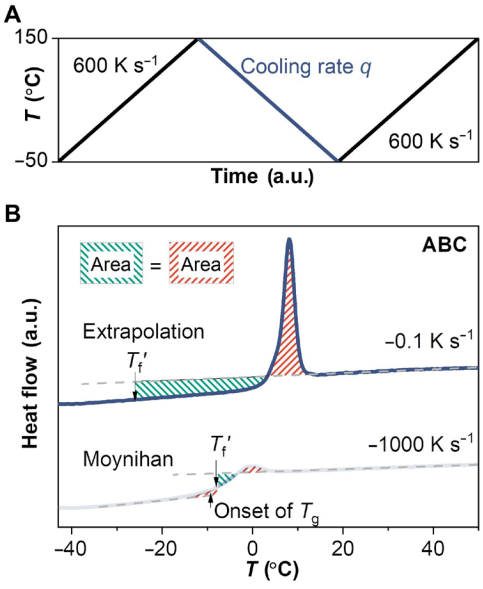

Fig. 3. FSC protocol used for all investigated materials and mixtures. (**A**) A sample is first heated to 150°C, then cooled at rate q ranging from −0.1 to −1000 K s^{-1}, and lastly heated again at 600 K s^{-1}. (**B**) T'_f was determined from the enthalpy overshoots in the heating scans by matching the green (\\\) and red (///) shaded areas according to the method by Moynihan *et al.* or by extrapolation (*31*–*33*), here illustrated for the ABC ternary mixture. a.u., arbitrary units.

For most systems, liquid-liquid transitions are typically accompanied by anomalies in thermodynamic variables such as the heat capacity C_p, thermal expansion coefficient, and isothermal compressibility (*38*). A comparison of FSC heating thermograms indicates that for single-component liquids, for instance, the heat flow above the glass transition is only weakly affected by the rate at which the material is cooled; i.e., the same liquid phase L_1 is maintained until the material vitrifies (fig. S5). Importantly, the heating scan of the octonary mixture obtained by slow cooling shows a larger heat flow until about 110°C than the more rapidly cooled material, indicating a new liquid state L_2 with a higher C_p, which gradually transitions into L_1, giving rise to a broad endotherm (fig. S5). We propose that multicomponent perylene mixtures that are cooled sufficiently slowly undergo a liquid-liquid transition from L_1 to L_2, and thus feature a lower fragility.

To elucidate the nature of the liquid-liquid transition of our perylene mixtures, we used variable-temperature photoluminescence (PL) spectroscopy. Perylenes exhibit different spectral signatures depending on their state of aggregation, with a pronounced red shift upon the formation of dimer-type structures (*46*–*48*). We studied the emission from thin films of the octonary mixture drop-cast from dichloromethane (DCM), sandwiched between two glass slides. The PL spectrum of the drop-cast octonary mixture features a broad peak at 590 nm, characteristic for aggregation (Fig. 5A), which we explain with the presence of excited complexes (exciplexes) (*46*). Note that the PL spectrum of the octonary mixture is distinct

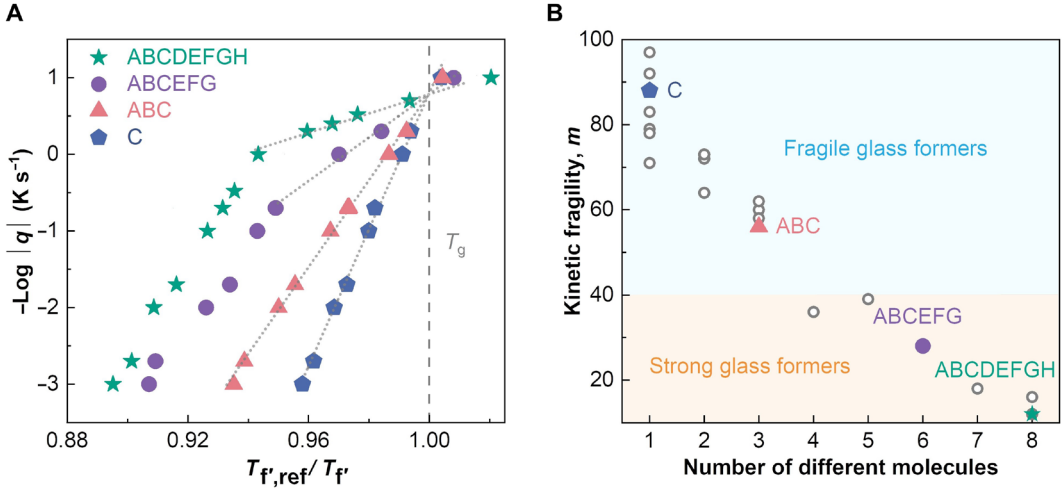

Fig. 4. Fragility plot. (**A**) −Log|q| versus $T'_{f,ref}/T'_f$, with T'_f from FSC for $q = -0.1$ to -1000 K s^{-1} and $T'_{f,ref}$ from DSC for $q = -0.17$ K s^{-1}, for a representative single-component C (pentagons), the ABC ternary (triangles), ABCEFG senary (circles), and ABCDEFGH octonary mixture (stars); the dotted lines are straight-line fits intersecting $T'_{f,ref} = T'_f$ from which fragility values m were calculated. (**B**) Kinetic fragility m as a function of the number of different perylene derivatives in the mixture; open circles correspond to measurements shown in figs. S3 and S4.

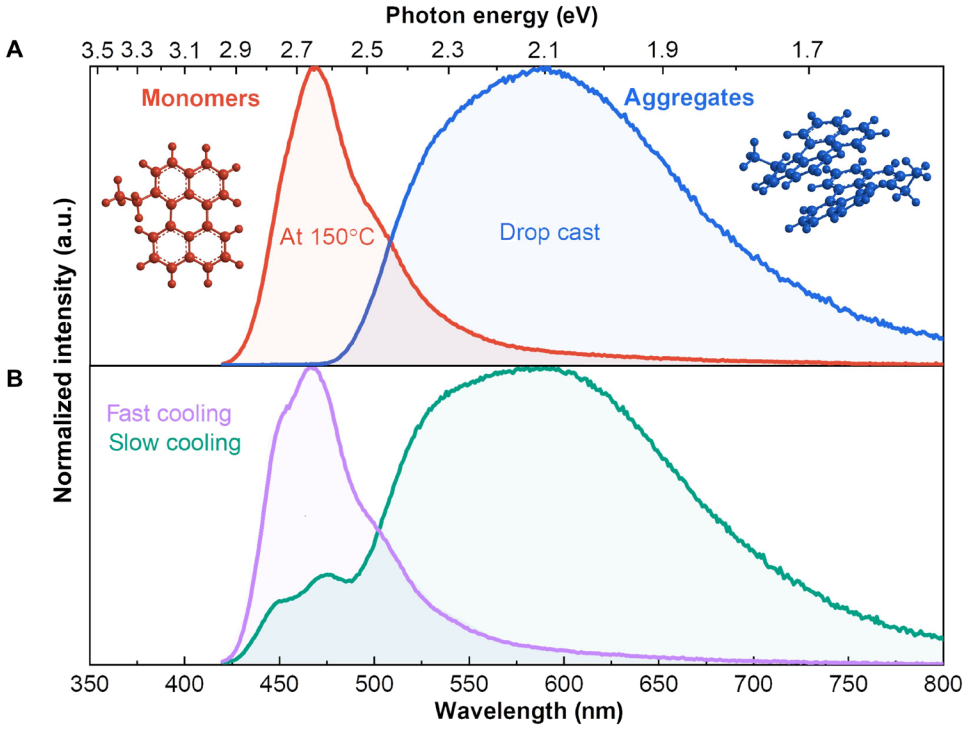

Fig. 5. PL spectroscopy. (**A**) Emission spectra of the octonary mixture directly after drop-casting (blue) and at 150°C (red). (**B**) Emission spectra taken at −40°C after fast and slow cooling from 150°C at a rate of −80 K s^{-1} (purple) or slow cooling at −0.1 K s^{-1} (green).

from those of, e.g., drop-cast films of molecule C, which has crystallized and gives rise to a sharp peak at 520 nm (fig. S6). Upon heating to 150°C, however, the emission shifts to 470 nm, which is typical for monomeric perylene (*46*) and characterizes liquid state L_1 (Fig. 5A). Fast cooling at –80 K s^{-1} leaves the PL spectrum unchanged, indicating that the perylene molecules do not have sufficient time to aggregate and hence the liquid state L_1 is maintained (Fig. 5B). In contrast, we observe a red shift of the emission to 590 nm upon cooling with a lower rate of –0.1 K s^{-1} (Fig. 5B), which indicates that the octonary mixture now has enough time to transform into liquid phase L_2 composed of aggregates (*46*). We conclude that the ability of perylenes to aggregate is rate dependent, which gives rise to the liquid-liquid transition that we infer for mixtures with more than three components (Fig. 4A and fig. S4).

DISCUSSION

We have studied the vitrification of mixtures of perylenes that feature alkyl groups at one of the bay positions. The here-studied mixtures of perylene derivatives do not readily crystallize, and their kinetic fragility decreases with the number of components. While individual derivatives are fragile glass formers with values of $m = 70$ to 90, mixtures with more than three components become strong glass formers with $m < 40$ (Fig. 4B). Octonary mixtures display a kinetic fragility as low as 13 ± 2, which is similar to the fragility of the prototype strong glass former SiO_2 whose viscosity follows Arrhenius behavior (*49*). This is a record low value for any glass-forming system investigated to date, including not only small organic molecules but also polymers and inorganic materials such as bulk metallic glasses and SiO_2. The low fragility arises because of a liquid-liquid transition from liquid phase L_1 to L_2 upon cooling, which is characterized by the formation of perylene aggregates. The liquid-liquid transition is only observed in mixtures of more than three bay-substituted perylenes. We therefore attribute the appearance of the liquid phase L_2 to the presence of a sufficient number of perylenes with different pendant groups.

We carried out density functional theory (DFT) calculations to understand the aggregates that make up L_2 in more detail. Pairs of molecules in planar configuration display a strong attractive interaction with a maximum binding energy of about 0.5 eV per perylene molecule in case of dimers with a slip-stack–type configuration (fig. S7). We argue that the aggregates that make up liquid phase L_2 are mixed stacks of perylenes, and hence, its entropy increases with the number of different molecules, which stabilizes L_2. Hence, we start to observe a liquid-liquid transition once the entropy of L_2 is sufficiently high, which is the case for mixtures with more than three components. The alkyl pendant groups of individual molecules in these stacks likely remain disordered. Therefore, the aggregates that make up liquid phase L_2 cannot serve as nuclei for crystallization, which would require reorganization of mixed stacks into monomolecular aggregates.

To illustrate the increase in the entropy of liquid phase L_2 with the number of derivatives, we first consider a single pair of perylene molecules. Because of the asymmetric nature of bay-substituted perylenes, there are several possible dimer configurations that only differ in the position of the pendant groups. Here, it is important to note that bay substitution results in twisting of the perylene core, and hence, each type of perylene (A to H) exists as a mixture of two distinct atropisomers, separated by an energy barrier of about 0.7 eV, which is sufficiently large to prevent interconversion (*29*). We first

consider a pair of molecules with the same pendant group. The same two atropisomers of perylene A can form two distinct AA dimer configurations (Fig. 6A), assuming that the pendant ethyl groups are positioned on opposite sides of the perylene dimer stack to minimize steric hindrance. On the other hand, two molecules with different pendant groups, e.g., one atropisomer each of perylenes A and B, give rise to four distinct AB dimers (Fig. 6B). Hence, a hypothetical liquid L_2 composed solely of dimers would have a higher entropy if it formed from a mixture of two different bay-substituted perylenes instead of a single perylene. DFT calculations show that the binding energies of AA and AB dimers are practically identical (0.5 eV per perylene molecule), meaning that aggregation of different types of perylene derivatives can occur.

It is likely that more than two bay-substituted perylene derivatives can associate to form an aggregate, leading to trimers, quadrimers, pentamers, etc. A multitude of aggregate configurations exists that differ not only in the number of molecules but also in the relative position of the pendant groups. Therefore, the entropy of liquid phase L_2 greatly increases with the number of components that make up the mixture. As a result, for multicomponent mixtures, there is a temperature window above T_g where the liquid phase L_2 is thermodynamically stable. For the octonary mixture, for example, there is a temperature window between $T_g \sim -17$°C and about 110°C where we observe the formation of the liquid phase L_2 (see the higher heat flow in FSC thermograms of the slowly cooled octonary mixture; fig. S5). At 150°C, the octonary mixture is in liquid phase L_1 that is composed of perylene monomers, which aggregate at lower temperatures provided that the material is cooled sufficiently slowly, giving rise to a liquid-liquid transition. Because the liquid phase L_2 is composed of aggregates, structural relaxation above the T_g requires collective motion of a large number of molecules, which reduces the fragility to the ultralow value of $m = 13 \pm 2$ observed for the octonary mixture.

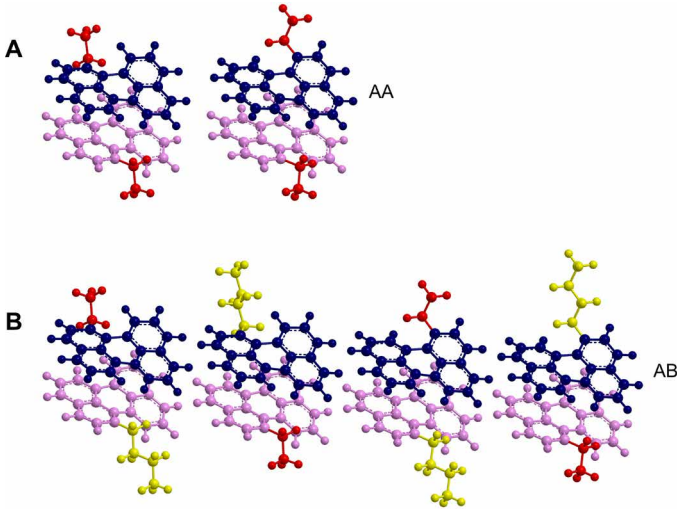

Fig. 6. Illustration of possible dimer configurations obtained from DFT calculations (see Materials and Methods). (**A**) Structures of the two possible AA dimer configurations incorporating the same two atropisomers of perylene A. (**B**) The four possible AB dimer structures based on the same atropisomer of A in combination with the same atropisomer of B; note that, for clarity, we exclude dimers where the pendant groups are positioned on the same side of the dimer, which have high energies due to a higher degree of steric hindrance.

In conclusion, the use of multicomponent mixtures of molecules can result in materials with a low fragility and hence strong tendency for glass formation. The kinetic fragility of the here-studied mixtures of perylene derivatives monotonously decreases with the number of components, reaching an ultralow fragility in the case of octonary mixtures, which provides a rationale for going beyond the usually studied binary or ternary systems of molecules. Mixtures of bay-substituted perylenes are of direct interest as liquid chromophores for solar energy storage and photon upconversion. In a broader context, glass-forming mixtures that undergo a liquid-liquid transition and thus avoid crystallization may open up new avenues for the design of organic semiconductors or pharmaceutical formulations, which could pave the way for more thermally stable organic solar cells and medicines with a longer shelf life.

MATERIALS AND METHODS

Materials

DCM and *o*-terphenyl were obtained from Sigma-Aldrich and used as received. All samples were prepared from equal weight ratios of the different components and processed from DCM solutions (10 g liter^{-1}). A description of the synthesis and characterization of molecules A, B, C, E, F, and G can be found in (*29*); the synthesis of molecules D and H is described in the Supplementary Materials, and their characterization with nuclear magnetic resonance, high-resolution mass spectrometry, and thin-layer chromatography is shown in figs. S8 to S12.

Differential scanning calorimetry

DSC measurements were carried out with a Mettler Toledo DSC2 equipped with a Gas controller GC 200 system. The perylene derivative was dissolved in DCM with a concentration of 10 g liter^{-1}, dried, and collected with tissue paper into a 40-µl Al crucible. Samples were first cooled down to −50°C at a rate of −10°C min^{-1} and kept isothermal for 30 min, followed by two heating/cooling cycles between −50° and 150°C at 10°C min^{-1}. Melting temperatures were extracted from the first heating scan, while the glass transition temperatures and the reference fictive temperatures were extracted from the second heating scan.

Fast scanning calorimetry

Measurements were conducted with a Mettler Toledo Flash DSC 1. A solution of perylene mixture (10 g liter^{-1}) in DCM was drop-cast on a glass substrate and dried, and a small amount of the material was transferred directly to the FSC chip sensor. The used FSC protocol is similar to those used in other studies (*32*, *33*). The sample was first heated to 150°C to delete the thermal history and then cooled down to −50°C with different cooling rates ranging from −0.1 to −1000 K s^{-1}. Last, the sample was heated at 600 K s^{-1} (see FSC protocol in Fig. 3A). To calculate the limiting fictive temperature T_f', we used Moynihan's area matching method, which is equal to Richardson's method in the Mettler Toledo software (Fig. 3B)

$$\int_{T_f}^{T \gg T_g} (C_{pl} - C_{pg})\, dT = \int_{T \ll T_g}^{T \gg T_g} (C_p - C_{pg})\, dT$$

where C_{pl} is the liquid heat capacity, C_{pg} is the glass heat capacity, and C_p is the apparent heat capacity of the sample. When T_f' was below the onset of devitrification, a simplified version was used

$$\int_{T_f'}^{T \gg T_g} (C_{pl} - C_{pg})\, dT = 0$$

Emission spectroscopy

A solution of perylene mixture (10 g liter^{-1}) in DCM was drop-cast on a glass substrate and dried, and another glass substrate was pressed on top to obtain a thin film. A LTS420 hotstage from Linkam Scientific Instruments Ltd. was used to heat and cool the sample. The sample was first heated to 150°C and then cooled to −40°C with fast and slow cooling. To obtain a fast-enough cooling, the sample was heated to 150°C on a heating plate, then cooled with liquid nitrogen, and measured at −40°C with the Linkam hotstage. Emission spectra were conducted using a spectrofluorometer (FLS1000, Edinburgh Instruments) at an excitation wavelength of 400 nm.

DFT calculations

Low-energy configurations and binding energies of AA dimer configurations were analyzed using DFT calculations, while AB dimer configurations were created by replacing one of the ethyl pendant groups of the calculated AA dimers with a butyl group without relaxing the perylene stack once more. Initial dimer configurations were generated by systematically rotating the two molecules relative to each other using tools from the Atomic Simulation Environment (*50*) and subsequently relaxed until the maximum force on any atom in the system was less than 10 meV Å^{-1}. Calculations were carried out using the B3LYP functional (*51*) with dispersion corrections (D3BJ) (*52*) and the 6–311G* basis set as implemented in the NWChem suite (*53*).

SUPPLEMENTARY MATERIALS

Supplementary material for this article is available at http://advances.sciencemag.org/cgi/content/full/7/29/eabi4659/DC1

REFERENCES AND NOTES

1. W. H. Wang, C. Dong, C. H. Shek, Bulk metallic glasses. *Mater. Sci. Eng. R* **44**, 45–89 (2004).
2. Y. Qiu, G. Zhang, Y. Chen, G. Zhang, L. Liu, W. Porter, *Developing Solid Oral Dosage Forms: Pharmaceutical Theory and Practice* (Elsevier Science & Technology, 2008).
3. M. T. Cicerone, J. F. Douglas, β-Relaxation governs protein stability in sugar-glass matrices. *Soft Matter* **8**, 2983–2991 (2012).
4. M. D. Ediger, Perspective: Highly stable vapor-deposited glasses. *J. Chem. Phys.* **147**, 210901 (2017).
5. C. Müller, On the glass transition of polymer semiconductors and its impact on polymer solar cell stability. *Chem. Mater.* **27**, 2740–2754 (2015).
6. J. A. Baird, B. Van Eerdenbrugh, L. S. Taylor, A classification system to assess the crystallization tendency of organic molecules from undercooled melts. *J. Pharm. Sci.* **99**, 3787–3806 (2010).
7. J. Shinar, *Organic Light-Emitting Devices: A Survey* (Springer, 2011).
8. A. Diaz de Zerio, C. Müller, Glass forming acceptor alloys for highly efficient and thermally stable ternary organic solar cells. *Adv. Energy Mater.* **8**, 1702741 (2018).
9. N. A. Mauro, M. Blodgett, M. L. Johnson, A. J. Vogt, K. F. Kelton, A structural signature of liquid fragility. *Nat. Commun.* **5**, 4616 (2014).
10. I. H. Bell, J. C. Dyre, T. S. Ingebrigtsen, Excess-entropy scaling in supercooled binary mixtures. *Nat. Commun.* **11**, 4300 (2020).
11. R. Böhmer, K. L. Ngai, C. A. Angell, D. J. Plazek, Nonexponential relaxations in strong and fragile glass formers. *J. Chem. Phys.* **99**, 4201–4209 (1993).
12. C. A. Angell, Formation of glasses from liquids and biopolymers. *Science* **267**, 1924–1935 (1995).
13. L.-M. Wang, C. A. Angell, R. Richert, Fragility and thermodynamics in nonpolymeric glass-forming liquids. *J. Chem. Phys.* **125**, 074505 (2006).
14. Q. Qin, G. B. McKenna, Correlation between dynamic fragility and glass transition temperature for different classes of glass forming liquids. *J. Non Cryst. Solids X* **352**, 2977–2985 (2006).
15. V. N. Novikov, Y. Ding, A. P. Sokolov, Correlation of fragility of supercooled liquids with elastic properties of glasses. *Phys. Rev. E* **71**, 061501 (2005).
16. K. Amann-Winkel, C. Gainaru, P. H. Handle, M. Seidl, H. Nelson, R. Böhmer, T. Loerting, Water's second glass transition. *Proc. Natl. Acad. Sci.* **110**, 17720–17725 (2013).
17. E. Kaminska, M. Tarnacka, K. Kaminski, K. L. Ngai, M. Paluch, Changes in dynamics of the glass-forming pharmaceutical nifedipine in binary mixtures with octaacetylmaltose. *Eur. J. Pharm. Biopharm.* **97**, 185–191 (2015).
18. K. Duvvuri, R. Richert, Binary glass-forming materials: Mixtures of sorbitol and glycerol. *J. Phys. Chem. B* **108**, 10451–10456 (2004).
19. A. Sanz, H. C. Wong, A. J. Nedoma, J. F. Douglas, J. T. Cabral, Influence of C60 fullerenes on the glass formation of polystyrene. *Polymer* **68**, 47–56 (2015).
20. H. Gong, M. Sun, Z. Li, R. Liu, Y. Tian, L.-M. Wang, Kinetic fragility of binary and ternary glass forming liquid mixtures. *Eur. Phys. J. E* **34**, 86 (2011).
21. L.-M. Wang, Y. Tian, R. Liu, R. Richert, Structural relaxation dynamics in binary glass-forming molecular liquids with ideal and complex mixing behavior. *J. Phys. Chem. B* **114**, 3618–3622 (2010).
22. L.-M. Wang, Z. Li, Z. Chen, Y. Zhao, R. Liu, Y. Tian, Glass transition in binary eutectic systems: Best glass-forming composition. *J. Phys. Chem. B* **114**, 12080–12084 (2010).
23. L.-M. Wang, Y. Zhao, M. Sun, R. Liu, Y. Tian, Dielectric relaxation dynamics in glass-forming mixtures of propanediol isomers. *Phys. Rev. E* **82**, 062502 (2010).
24. K. Grzybowska, M. Paluch, P. Wlodarczyk, A. Grzybowski, K. Kaminski, L. Hawelek, D. Zakowiecki, A. Kasprzycka, I. Jankowska-Sumara, Enhancement of amorphous celecoxib stability by mixing it with octaacetylmaltose: The molecular dynamics study. *Mol. Pharm.* **9**, 894–904 (2012).
25. C. Liu, Z. Liu, X. Yin, G. Wu, Tuning the dynamic fragility of acrylic polymers by small molecules: The interplay of hydrogen bonding strength. *Macromolecules* **48**, 4196–4206 (2015).
26. C. Dalle-Ferrier, S. Simon, W. Zheng, P. Badrinarayanan, T. Fennell, B. Frick, J. M. Zanotti, C. Alba-Simionesco, Consequence of excess configurational entropy on fragility: The case of a polymer-oligomer blend. *Phys. Rev. Lett.* **103**, 185702 (2009).
27. R. A. Riggleman, J. F. Douglas, J. J. d. Pablo, Tuning polymer melt fragility with antiplasticizer additives. *J. Chem. Phys.* **126**, 234903 (2007).
28. R. Yue, Y. Niu, Z. Wang, J. F. Douglas, X. Zhu, E. Chen, Suppression of crystallization in a plastic crystal electrolyte (SN/$LiClO_4$) by a polymeric additive (polyethylene oxide) for battery applications. *Polymer* **50**, 1288–1296 (2009).
29. K. Kushwaha, L. Yu, K. Stranius, S. K. Singh, S. Hultmark, M. N. Iqbal, L. Eriksson, E. Johnston, P. Erhart, C. Müller, K. Börjesson, A record chromophore density in high-entropy liquids of two low-melting perylenes: A new strategy for liquid chromophores. *Adv. Sci.* **6**, 1801650 (2019).
30. F. Würthner, C. R. Saha-Möller, B. Fimmel, S. Ogi, P. Leowanawat, D. Schmidt, Perylene bisimide dye assemblies as archetype functional supramolecular materials. *Chem. Rev.* **116**, 962–1052 (2016).
31. C. T. Moynihan, A. J. Easteal, M. A. De Bolt, J. Tucker, Dependence of the fictive temperature of glass on cooling rate. *J. Am. Ceram. Soc.* **59**, 12–16 (1976).
32. S. Gao, Y. P. Koh, S. L. Simon, Calorimetric glass transition of single polystyrene ultrathin films. *Macromolecules* **46**, 562–570 (2013).
33. R. Tao, E. Gurung, M. M. Cetin, M. F. Mayer, E. L. Quitevis, S. L. Simon, Fragility of ionic liquids measured by Flash differential scanning calorimetry. *Thermochim. Acta* **654**, 121–129 (2017).
34. S. Gao, S. L. Simon, Measurement of the limiting fictive temperature over five decades of cooling and heating rates. *Thermochim. Acta* **603**, 123–127 (2015).
35. K. Ito, C. T. Moynihan, C. A. Angell, Thermodynamic determination of fragility in liquids and a fragile-to-strong liquid transition in water. *Nature* **398**, 492–495 (1999).
36. I. Saika-Voivod, P. H. Poole, F. Sciortino, Fragile-to-strong transition and polyamorphism in the energy landscape of liquid silica. *Nature* **412**, 514–517 (2001).
37. M. Hemmati, C. T. Moynihan, C. A. Angell, Interpretation of the molten BeF2 viscosity anomaly in terms of a high temperature density maximum, and other waterlike features. *J. Chem. Phys.* **115**, 6663–6671 (2001).
38. P. Lucas, G. J. Coleman, M. Venkateswara Rao, A. N. Edwards, C. Devaadithya, S. Wei, A. Q. Alsayoud, B. G. Potter, K. Muralidharan, P. A. Deymier, Structure of ZnCl2 melt. Part II: Fragile-to-strong transition in a tetrahedral liquid. *J. Phys. Chem. B* **121**, 11210–11218 (2017).
39. C. Zhang, L. Hu, Y. Yue, J. C. Mauro, Fragile-to-strong transition in metallic glass-forming liquids. *J. Chem. Phys.* **133**, 014508 (2010).
40. S. Wei, P. Lucas, C. A. Angell, Phase change alloy viscosities down to Tg using Adam-Gibbs-equation fittings to excess entropy data: A fragile-to-strong transition. *J. Appl. Phys.* **118**, 034903 (2015).
41. C. Way, P. Wadhwa, R. Busch, The influence of shear rate and temperature on the viscosity and fragility of the $Zr_{41.2}Ti_{13.8}Cu_{12.5}Ni_{10.0}Be_{22.5}$ metallic-glass-forming liquid. *Acta Mater.* **55**, 2977–2983 (2007).

42. S.-X. Peng, Y. Cheng, J. Pries, S. Wei, H.-B. Yu, M. Wuttig, Uncovering β-relaxations in amorphous phase-change materials. *Sci. Adv.* **6**, eaay6726 (2020).
43. P. Lucas, Fragile-to-strong transitions in glass forming liquids. *J. Non Cryst. Solids X* **4**, 100034 (2019).
44. Q. Sun, C. Zhou, Y. Yue, L. Hu, A direct link between the fragile-to-strong transition and relaxation in supercooled liquids. *J. Phys. Chem. Lett.* **5**, 1170–1174 (2014).
45. R. Shi, J. Russo, H. Tanaka, Origin of the emergent fragile-to-strong transition in supercooled water. *Proc. Natl. Acad. Sci.* **115**, 9444–9449 (2018).
46. C. Ye, V. Gray, K. Kushwaha, S. Kumar Singh, P. Erhart, K. Börjesson, Optimizing photon upconversion by decoupling excimer formation and triplet triplet annihilation. *Phys. Chem. Chem. Phys.* **22**, 1715–1720 (2020).
47. R. Katoh, S. Sinha, S. Murata, M. Tachiya, Origin of the stabilization energy of perylene excimer as studied by fluorescence and near-IR transient absorption spectroscopy. *J. Photochem. Photobiol. A* **145**, 23–34 (2001).
48. R. E. Cook, B. T. Phelan, R. J. Kamire, M. B. Majewski, R. M. Young, M. R. Wasielewski, Excimer formation and symmetry-breaking charge transfer in cofacial perylene dimers. *J. Phys. Chem. A* **121**, 1607–1615 (2017).
49. K. F. Kelton, Kinetic and structural fragility - A correlation between structures and dynamics in metallic liquids and glasses. *J. Phys. Condens. Matter* **29**, 023002 (2016).
50. A. H. Larsen, J. J. Mortensen, J. Blomqvist, I. E. Castelli, R. Christensen, M. Dułak, J. Friis, M. N. Groves, B. Hammer, C. Hargus, E. D. Hermes, P. C. Jennings, P. B. Jensen, J. Kermode, J. R. Kitchin, E. L. Kolsbjerg, J. Kubal, K. Kaasbjerg, S. Lysgaard, J. B. Maronsson, T. Maxson, T. Olsen, L. Pastewka, A. Peterson, C. Rostgaard, J. Schiøtz, O. Schütt, M. Strange, K. S. Thygesen, T. Vegge, L. Vilhelmsen, M. Walter, Z. Zeng, K. W. Jacobsen, The atomic simulation environment-a Python library for working with atoms. *J. Phys. Condens. Matter* **29**, 273002 (2017).
51. C. Lee, W. Yang, R. G. Parr, Development of the Colle-Salvetti correlation-energy formula into a functional of the electron density. *Phys. Rev. B* **37**, 785–789 (1988).
52. S. Grimme, J. Antony, S. Ehrlich, H. Krieg, A consistent and accurate ab initio parametrization of density functional dispersion correction (DFT-D) for the 94 elements H-Pu. *J. Chem. Phys.* **132**, 154104 (2010).
53. M. Valiev, E. J. Bylaska, N. Govind, K. Kowalski, T. P. Straatsma, H. J. J. Van Dam, D. Wang, J. Nieplocha, E. Apra, T. L. Windus, W. A. de Jong, NWChem: A comprehensive and scalable open-source solution for large scale molecular simulations. *Comput. Phys. Commun.* **181**, 1477–1489 (2010).

Acknowledgments: We thank A. Matic for highly insightful comments. **Funding:** S.H. and C.M. gratefully acknowledge support from the Knut and Alice Wallenberg Foundation through the project "Mastering Morphology for Solution-borne Electronics". K.B. gratefully acknowledges financial support from the European Research Council (ERC-2017-StG-757733). P.E. gratefully acknowledges financial support from the Swedish Research Council (2020-04935). The computations were enabled by resources provided by the Swedish National Infrastructure for Computing (SNIC) at NSC, C3SE, and PDC partially funded by the Swedish Research Council (grant number 2018-05973). **Author contributions:** S.H. designed and performed all thermal analyses and PL measurements and analyzed the data with input from C.M. and K.B. A.C., K.K., and S.M. synthesized the bay-substituted perylenes under the supervision of K.B. P.E. carried out the DFT calculations. S.H. and C.M. designed the study, planned the experiments, and wrote the manuscript. All coauthors assisted with writing and editing of the manuscript. **Competing interests:** The authors declare that they have no competing interests. **Data and materials availability:** All data needed to evaluate the conclusions in the paper are present in the paper and/or the Supplementary Materials or can be accessed via DOI: 10.5281/zenodo.4880209. Additional data related to this paper may be requested from the authors.

Submitted 11 March 2021
Accepted 2 June 2021
Published 16 July 2021
10.1126/sciadv.abi4659

Citation: S. Hultmark, A. Cravcenco, K. Kushwaha, S. Mallick, P. Erhart, K. Börjesson, C. Müller, Vitrification of octonary perylene mixtures with ultralow fragility. *Sci. Adv.* **7**, eabi4659 (2021).

Science Advances

Vitrification of octonary perylene mixtures with ultralow fragility

Sandra Hultmark, Alex Cravcenco, Khushbu Kushwaha, Suman Mallick, Paul Erhart, Karl Börjesson and Christian Müller

Sci Adv **7** (29), eabi4659.
DOI: 10.1126/sciadv.abi4659